Visual Abstract

Predicting the lifetime of CPVC under increasing temperature and crosshead speed

Abderrahim Khtibari, Abdelkrim Kartouni, Mohamed Elghorba
Condensed Matter Physics Laboratory, Faculty of Sciences Ben M'Sick, University Hassan of Casablanca, B.P. 7955, Casablanca, Morocco
khtibarii@gmail.com, krimkart@gmail.com, medelghorba2@gmail.com

Abderrazak En-Naji
Laboratory M3ER, Sciences Faculty and Technology, Moulay Ismail University, Meknes, Morocco
abdenaji14@gmail.com

Abstract. The aim of this paper is to characterize the mechanical characteristics of chlorinated PVC (CPVC). Tensile tests were carried on the compounds at different temperatures ranging from -20 to 90°C and crosshead speeds from 5 to 500 mm/min. The results were analyzed to determine how crosshead speed and temperature affected on the mechanical characteristics of CPVC specimens. Two damage models are then developed, one model obtained by adapting the unified theory version and the other quasi-experimental static model based on ultimate stress. These models allow us to evaluate the damage evolution of CPVC samples and to determine the safety and maintenance intervals of this material.

Keywords. CPVC, Temperature, Crosshead speed, Damage, Unified theory.

Citation: Khtibari, A., Kartouni, A., Elghorba, M., En-Naji, A., Predicting the lifetime of CPVC under increasing temperature and crosshead speed, Frattura ed Integrità Strutturale, 66 (2023) 140-151.

Received: 12.06.2023
Accepted: 12.08.2023
Online first: 15.08.2023
Published: 01.10.2023

Introduction

Recently, due to its beneficial physical and chemical properties, such as temperature, corrosion, and impact resistance, chlorinated polyvinyl chloride (CPVC) has been widely used in industries for water, wastewater, and gas transportation [1]. The CPVC is also less expensive when compared with the copper [2]. This polymer is produced through a post-chlorination process that raises the chlorine content from 57.4% in PVC to 70% in CPVC [3]. This modification is intended to raise the glass transition temperature T_g of the base resin from 95°C to 115–135°C and improves its mechanical characteristics at elevated temperatures [4]. The CPVC pipes have higher temperature and pressure rating than PVC pipes, making them suitable for hot water delivery systems and other applications requiring higher temperatures and pressure ratings [5]. For this reason, studying the mechanical properties and damage of the polymer material is essential to avoiding partial and total fracture [6]. The knowledge gained from these studies can be used to improve the design,

manufacture, and maintenance of these materials, as well as the safety of their utilization [7]. Many efforts have been devoted to studying the main parameters that affect the mechanical behaviors of polymers and the CPVC material [8]. Joshi et al, observing and reported an improvement in the mechanical characteristics of PVC as a function of graphene oxide loading. Both the yield stress and elastic modulus were increased during this loading [9]. Merah and his team studied the effect of temperature on the mechanical behavior of CPVC pipe. The study's findings demonstrated that the Young's modulus and yield stress decreased as the temperature increased [10]. Liao et al. examined the tensile deformation and tensile failure behavior of transparent polyurethane under a range of temperature and strain rate conditions. Tensile tests were conducted on samples of polyurethane at various temperatures and strain rates. The results showed that the strain rate and temperature had a significant effect on the tensile deformation and failure of the polyurethane. At higher strain rates, a greater amount of strain was observed compared to lower strain rates, while higher temperatures resulted in greater plasticity and strain recovery [11]. Reis et al, analyzed the influence of temperature and strain rate on the mechanical properties of recycled HDPE. The authors found that changes in temperature and strain rate can significantly alter the tensile behavior of recycled HDPE. Moreover, the results suggest that temperature changes have a larger effect than strain rate changes on the tensile behavior of HDPE [12]. In a study conducted by Kendall et al, the temperature and strain rate dependance in PVC were showed that the temperature and crosshead speeds have a significant impact on the mechanical characteristics such as yield strength and Yong's modulus. These parameters decrease with increasing temperature and increase with increasing strain rate [13]. En-naji et al, examined the properties of ABS polymer plate subjected to uniaxial loading. The authors employed a standardized damage model to characterize the underlying mechanical behavior of the plate [14]. Plaseied and Fatemi examined the effects of strain rate and temperature on the tensile properties of a vinyl ester polymer. The results of tensile tests conducted at a range of strain rates and temperatures are used to analyze the effects of these factors on the mechanical properties of the material [15]. Yang et al, investigated the temperature and strain rate sensitivity of the yield strength of amorphous polymers. The researchers aimed to characterize and model the influence of temperature and strain rate on the yield strength of these materials. To this end, a series of experiments were conducted to determine the temperature and strain rate sensitivity of the yield strength of polycarbonate, polybutylene terephthalate, and polymethyl methacrylate [16]. Gugouch et al. explored how the fracture properties of CPVC pipes with defects are affected by burst pressure and predicted the fraction of life that these pipes can be expected to survive. The authors discussed the types of defects that can occur in CPVC pipes and the effects that these defects can have on their fracture properties. They also examined how burst pressure affects the fracture properties of CPVC pipes and the fraction of life that these pipes can be expected to survive [17]. Khtibari et al. examined the effect of strain rate on the damage of CVPC compound at room temperature. They found that the damage of the CVPC compound increases with an increasing strain rate. These findings could be used to improve the design and manufacture of CVPC compounds and to develop materials with enhanced resistance to high strain rate loading [18]. In this context, we choose to characterize the mechanical characteristics of chlorinated PVC (CPVC) due to their applications. For this raison, tensile tests were carried on the compounds at different temperatures ranging from -20 to 90°C and crosshead speeds from 5 to 500 mm/min. The results were analyzed to determine how crosshead speed and temperature affected on the mechanical characteristics of CPVC specimens. Two damage models were developed, one obtained by adapting the unified theory version and the other a quasi-experimental static damage based on ultimate stress. These models allow us to evaluate the damage evolution of CPVC samples and to determine the safety and maintenance intervals of this material.

EXPERIMENTAL PROCEDURE

The aim of the tensile testing is to identify the tensile characteristics of the CPVC specimens. Tensile testing is used to measure the amount of stress that can be applied to a material before it breaks or deforms permanently [19]. This information is useful for engineers and manufacturers to determine the suitability of a material for a particular application or product [20]. To do this, the samples for tensile test were used 10.16 cm schedule 80 CPVC pipes with a 9.5 mm wall thickness, these values obtained from commercial sources. 50 mm wide rings were cut from the pipes and slit to be flattened, as illustrated in Fig. 1. Following this, they were heated in an electric oven at 120°C for 65 minutes, then straightened in a designed mold shown in Fig. 2.

The straightened plates were then used to fabricate the components. The machining process was completed using coolants to avoid any damage to the material caused by the heat created. Samples have been prepared according to the ASTM D638-01 standard (Fig. 3). The dimensions and geometry of the tensile compounds used in this work are illustrated in Fig. 4. We used an Instron 8501 material. The system's primary control modes are load (±100 kN), strain (±10%), and position (±75 mm).

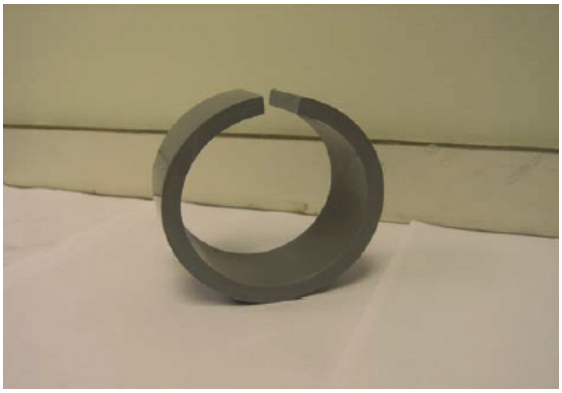

Figure 1: Ring width equal fifty millimeters was cut from CPVC pipe.

Figure 2: Designed mold for straightening compounds.

Figure 3: The CPVC specimen.

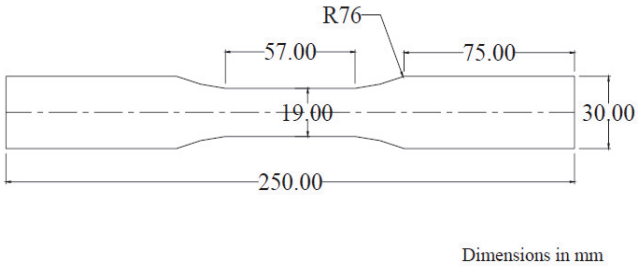

Figure 4: Dimension and geometry of the tensile compound used in the work.

Users of the control limits can be view on the digital control panel at any time during the test. Fig. 5 shows a photograph of the testing frame with an environmental chamber and video camera. Throughout the test, specially machined inserts were used to verify the samples vertical alignment. At each of these temperatures -20, 0, 10, 25, 50, 70, and 90°C, and at three crosshead speeds 5, 50 and 500 mm.min^{-1}, three tensile tests were performed. The results of the tests presented in the subsequent section.

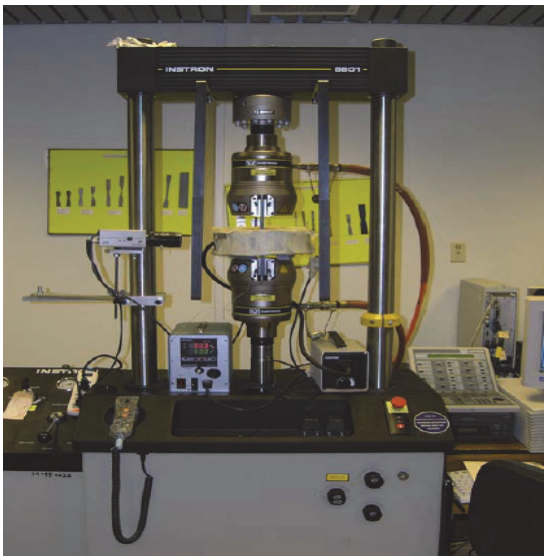

Figure 5: Thermal environmental chamber.

RESULTS AND DISCUSSION

Effects of temperature and crosshead speed on tensile properties

The stress-strain curve of chlorinated polyvinyl chloride (CPVC) is an important indicator of its mechanical properties and performance. Investigating the stress-strain curves of CPVC at various crosshead speeds and temperatures can help us to gain a better understanding of the material's behavior. Fig. 7, illustrates the evolution of the nominal stress-strain relationship according to these two parameters.

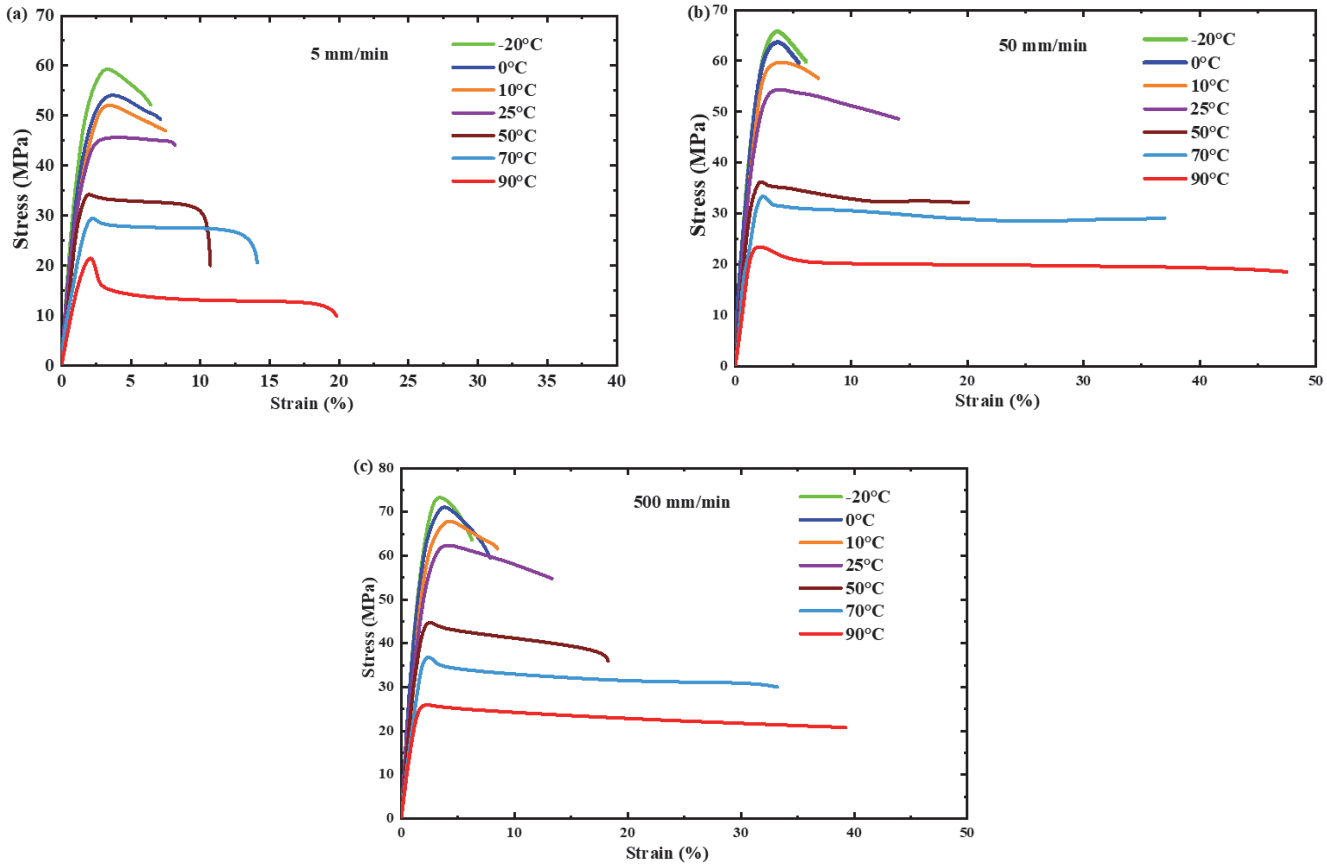

Figure 6: The nominal Stress-Strain of Chlorinated Polyvinyl Chloride were investigated at various crosshead speeds ranging 5(a), 50(b) and 500(c) mm/min, and temperatures ranging from -20 to 90°C.

It is evident that the effects of temperature and crosshead speed on CPVC's stress-strain characteristics are significant. The results of the tensile tests indicate that brittle fracture occurs at temperatures below 25°C and ductile fracture appears at temperatures above that. At lower temperatures (-20, 0 and 10°C), there is less strain energy available to deform the CPVC material, making it easier for a fracture to occur, while at temperatures between 50 and 90°C, the plastic behavior is predominant because the material has more energy available to deform and bend before it breaks, making it more ductile [21]. From the Fig. 6, the important features such as yield stress and elastic modulus can be determined. The impacts of the temperature and the crosshead speed on the median values of these two mechanical characteristics are displayed in Figs. 7, 8, 9 and 10. The evolution of the median yield stress with various crosshead speed and the temperatures is shown in Fig. 7. Fig. 7 shows that the value of yield stress increases logarithmically with increasing of the crosshead speed. In detail, as crosshead speed increases from 5 to 500 mm/min, the average yield strength increases from around 46 MPa to around 60 MPa at room temperature. The increase of yield strength can be explained by the decreased molecular mobility due to the short time available for the plastic zone, resulting in low ductility [10, 11]. The variation of yield strength with various temperatures is illustrated in Fig. 8.

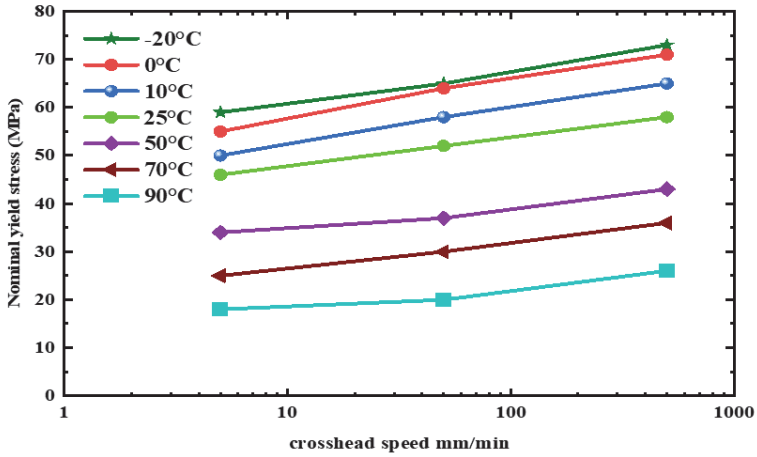

Figure 7: Tensile nominal yield stress with various crosshead speed.

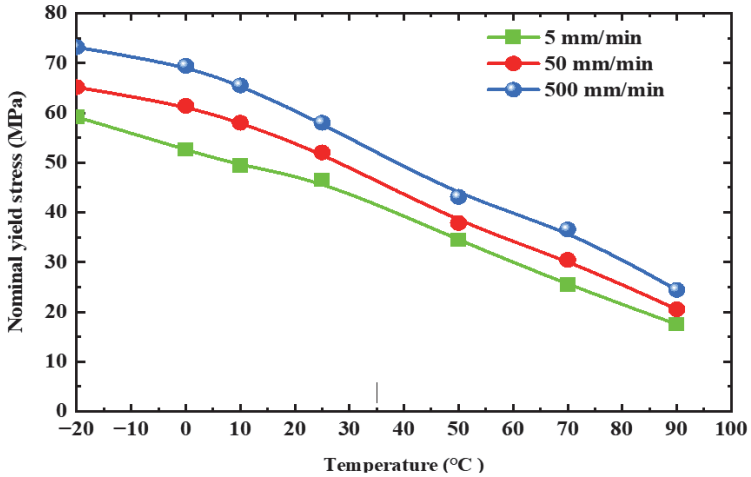

Figure 8: Tensile nominal yield stress with various temperature.

From Fig. 8, we can note that as the temperature increased from -20°C to 90°C at 5 mm/min, the yield strength of the material decreased drastically from 59.18 to 18.50 MPa. This can be attributed to the increased molecular mobility at higher temperatures, making it easier for the molecules to move and become more malleable under stress. Additionally, plastic deformation of the CPVC material is more likely to occur at higher temperatures due to the increased mobility of the molecules, further reducing the yield stress [21]. The median values of elastic modulus CPVC as a function of crosshead speed are displayed in Fig. 9.

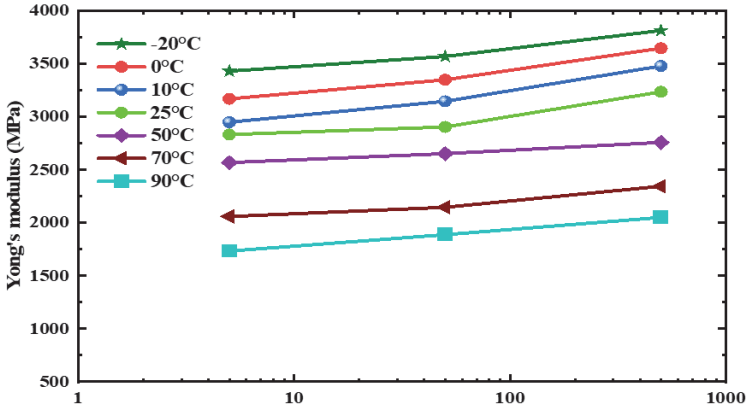

Figure 9: Tensile Young's modulus with various crosshead speed.

From this figure, we can see that the value of Young's modulus increases logarithmically with crosshead speed . The higher crosshead speed causes more molecules to become aligned, which increases the stiffness of the material [22]. The results of the study on the impact of temperature on Young's modulus for CPVC at various crosshead speed are clearly visible in Fig. 10. It is shown that the elastic modulus decreases linearly with increasing temperature. At temperatures below room temperature (i.e., -20, 0 and 10°C), the elastic modulus is relatively high. As the temperature continues to rise, however, the elastic modulus decreases, leading to an increase in the free volume between the chain molecules which further enables longer chain motion. As evidenced by the data, at high temperatures of 50, 70 and 90°C, the elastic modulus is significantly lower compared to those at lower temperatures. Unsurprisingly, this decrease in elastic modulus leads to increased flexibility of the material. [23].

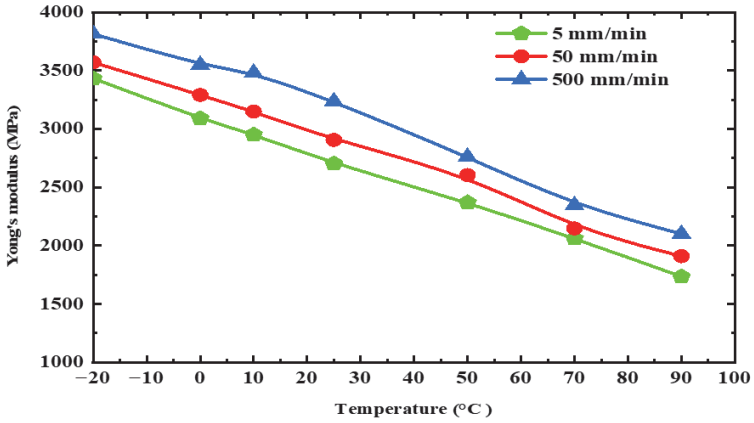

Figure 10: Tensile Young's modulus with various temperature.

Experimental Damage

Permanent damage of material leads to the reduction on mechanical properties, resulting in a reduced static tensile strength and fracture energy [24, 25]. If not properly maintained or repaired, the damage can lead to decrease in the functionality and performance of material, and eventually, to the breakdown of the material [26]. To this end, the ERISMANN model [27] has been proposed, which models damage in terms of certain physical parameters (e.g., load drop, ultimate stress, and modulus of elasticity...) at any point in material's life cycle, as described by the following equation [28]:

$$D=\frac{\Phi(x)-\Phi(x_O)}{\Phi(x_R)-\Phi(x_O)} \quad (1)$$

Φ(x): a monotonic function of x that is precisely defined.
x: the value the damage to the property.
O: start life material and R: End life material.
The function ϕ is used to represent the variation of some characteristics including load drop, ultimate stress, and modulus of elasticity, etc. According to the ERISEMANN law, it can be observed that the variation of the residual ultimate stress is represented by the function ϕ, and x denotes the life fraction β. This, in turn gives the static damage by ultimate stress with the following expression: $\phi(x) = \sigma_{ur}$.

$$D=\frac{\sigma_{ur}-\sigma_u}{\sigma_a-\sigma_u} \quad (2)$$

σ_a is the value of ultimate stress in MPa at 90°C.
σ_{ur} is the residual ultimate stress in MPa.
σ_u is the ultimate stress in MPa.
The results of the damage quantification based on the ultimate residual stress values are promising. By fitting the two different damage laws with the stress method, the varying degrees of damage stages can be accurately identified and

validated. This information, in turn, can be used to inform future research on failure prediction under realistic loading conditions. Ultimately, this could help improve the accuracy of structural models and optimize engineering designs.
Fig. 11 demonstrates the evolution of experimental damage based on ultimate stress in function according to life fraction β [14-29].

$$\beta = \frac{T_f - T_i}{T_f - T_{-20°C}} \tag{3}$$

where $T_{-20°C}$ is the temperature value at -20°C, T_i instantaneous temperature, and T_f the highest temperature.

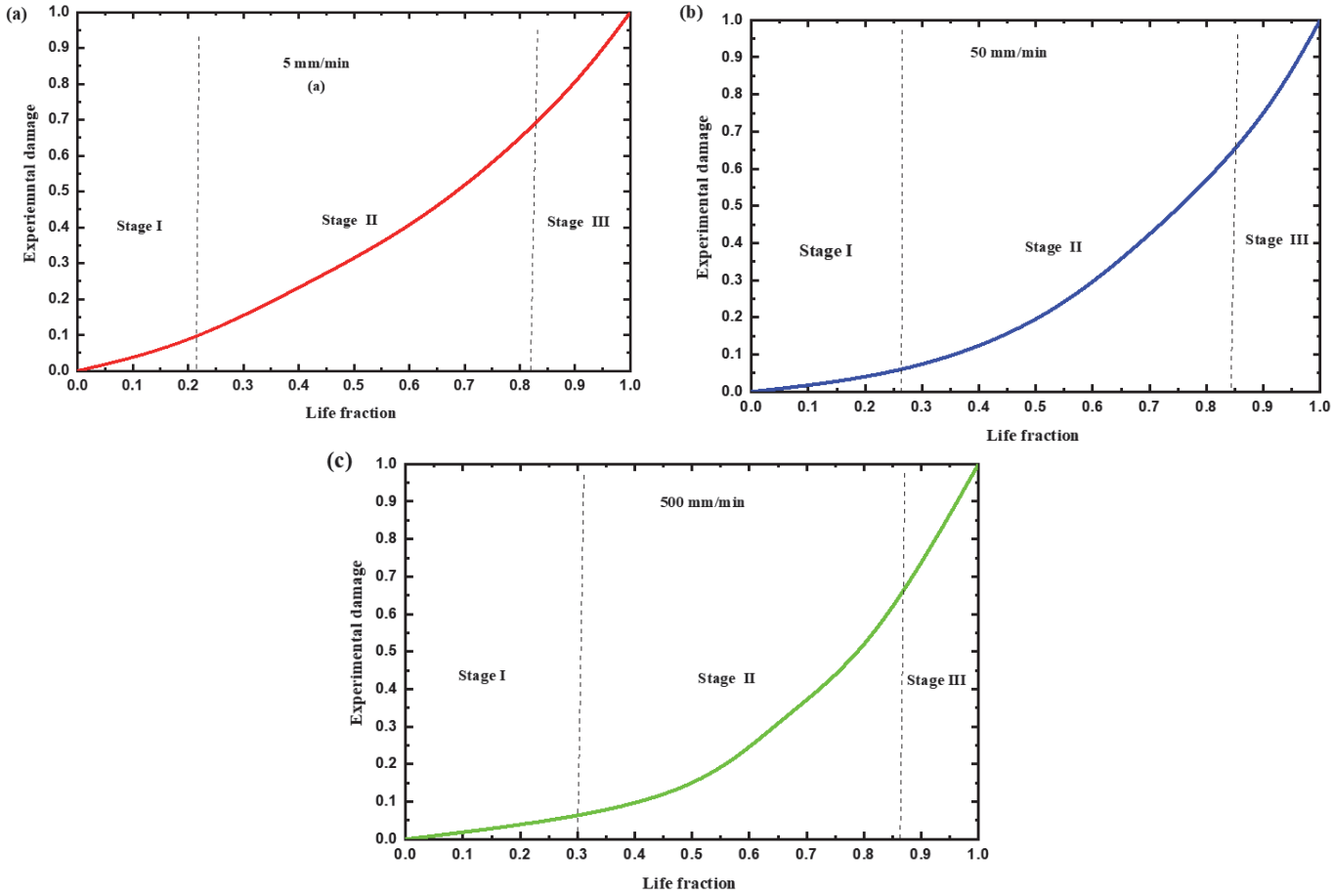

Figure 11: Variation of experimental damage with different temperature and crosshead speed ranging 5(a), 50(b) and 500(c) mm/min.

This figure shows the evolution of damage in CPVC polymer over the life fraction β. As can be seen, the damage increases with increasing β for given strain rate, indicating that the material is becoming increasingly brittle. The figure shows that the damage increases significantly at different life fractions for different crosshead speed, indicating that the material is highly strain rate dependent. We also note that as the fraction of life increases, the amount of damage done to the sample increases, resulting in a decrease in the static tensile strength. This decrease is gradual because the material is slowly being worn down until it eventually fails to resist the applied stress. The same figure allowed us to deduce the progression of damage in three stages, depending on the change in curvature. The first stage when the curve is linear, corresponding to its initiation for a fraction of life less than 20, 26 and 30%, respectively, when the crosshead speed is changed to 5 (a), 50 (b), and 500 (c) mm/min. In this stage the damage grows slowly, and the test tube begins to lose its internal. The second stage of damage occurs when the life fraction is found in the intervals [20- 80%] (when the crosshead speed is set to 5 mm/min), [26 - 84%] (when the crosshead speed is set to 50 mm/min), and [30 - 88%] (when the crosshead speed is set to 500 mm/min). In this stage, the damage is more severe, and the structure may still be safe with certain repairs and modifications. Also, at this stage, the damage becomes progressive and dangerous, so predictive maintenance is required on the industrial side to prevent any accidental service disruption. At the third stage, when the life fraction exceeds 80%, 84%, and 88% respectively of

5, 50 and 500 mm/min. In this context, the damages are critical, and the structure may no longer be safe. At this point, the structure may need to be completely replaced.

Damage and Reliability Relationship

The performance of system is determined by two key factors: damage D and reliability R. Damage D is a measure of the physical wear and tear a system may experience, whereas reliability R is a measure of a system's ability to function as expected over a given period of time. The lifetime of the system can be characterized by a combination of these two parameters and can be used to estimate how long the system can be expected to last before needing to be serviced or replaced [30]. Since these two parameters are complementary in nature, they can be expressed in the form of an equation.

$$R(\beta) = 1 - D(\beta) \tag{4}$$

In this equation, R symbolizes reliability and D represents damage. Moreover, the value of 1 is a mean that both parameters must always be present to accurately study a system's lifetime. The Eqn. (3) permits us to plot the reliability-damage curves according to the various life fraction (Fig. 12).

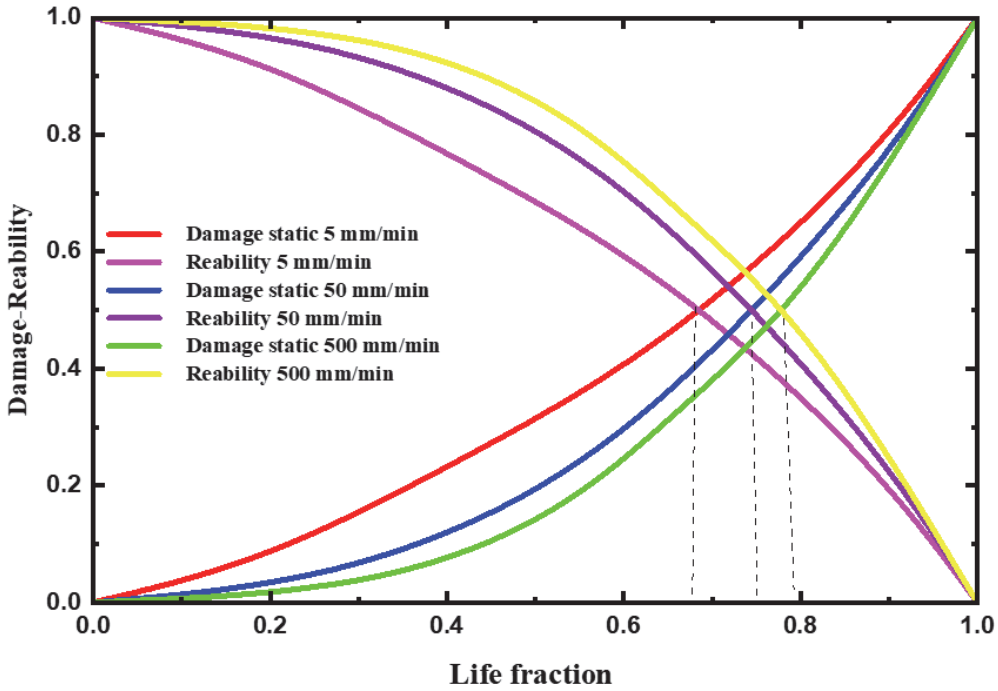

Figure 12: Reliability and damage curves of CPVC.

From the Fig. 12, we observe that reliability decreases while damage increases. The intersection between these two models allows us to determine the critical life fraction βc values, respectively are βc5 = 68%, βc50 =76%, and βc500 =80%. We note that as the crosshead speed increases, the critical life fraction value also increases. This is because the higher velocity of crosshead, the higher the strength and the lower the damage value [31]. Note that when the life fraction becomes critical, predictive maintenance must be planned to avoid total failure of this material.

Unified theory model

One of the first law was Miner's, which was created in 1945 [32]. The underlying assumption of this law is that cumulative damage in materials evolves linearly with life fraction and is unaffected by loading levels. Bui-Quoc's groundbreaking unified theory incorporates the theory of Henry, Gatts, Shanley, and Valluri to encompass a macroscopic perspective of damage accumulation [33]. The unified model is defined as follows [34]:

$$D=\frac{\beta}{\beta+(1-\beta)\left[\frac{\gamma-\left(\frac{\gamma}{\gamma_u}\right)^m}{\gamma-1}\right]} \quad (5)$$

with:

$\gamma= \sigma_{ur} /\sigma_u$ and $\gamma_u= \sigma_u /\sigma_a$

β: denotes the life fraction.

m = 0.98: represents a constant material.

Fig. 13 shows a series of curves representing the damage versus life fraction for various loading levels of γ. This parameter employed to measure the material's response on mechanical load when applied varied levels at temperature and crosshead speed. It helps to determine the safety and maintenance intervals of this material as presented in the Tab.. 1.

Crosshead speeds (mm/min)	Maximum load level (γ)	Minimum load level (γ)
5	2.3	1.2
50	2.8	1.3
500	3	1.8

Table 1: The maximum and minimum load level values at 5, 50, and 500 mm/min.

As seen in the Fig. 13 and Tab. 1, the maximum concavity is observed for the loading levels of γ = 1.2, 1.3, and 1.8 at 5, 50, and 500 mm/min respectively. It is evident that as the loading level rises, the damage caused by the curve is becoming more and more similar to the damage caused by the Miner linear model. We can distinguish the three stages of damage due to the alteration of the curvature. The beginning of damage for a zone life fraction begins at 0-22%, 0-26%, and 0-28%, respectively, when the crosshead speed is changed to 5 (a), 50 (b), and 500 (c) mm/min. The second stage of damage propagation, which is particular importance in the industrial applications, it was found in the intervals [22 - 82%] (when the crosshead speed is set to 5 mm/min), [26 - 85%] (when the crosshead speed is set to 50 mm/min), and [28- 87%] (when the crosshead speed is set to 500 mm/min). The third stage of the damage accumulation process is particularly significant, as it is responsible for critical damage that requires predictive maintenance. It was found that the critical life fraction during this stage was highly dependent on crosshead speed, with values of 82%, 85%, and 88% observed for 5 mm/min (a), 50 mm/min (b), and 500 mm/min (c), respectively. Notably, the damage during this stage accelerates suddenly to reach a value of unity and can result in sudden rupture, leaving the specimen useless. Therefore, due to its drastic and unpredictable nature, this stage requires extra attention when it comes to predictive maintenance.

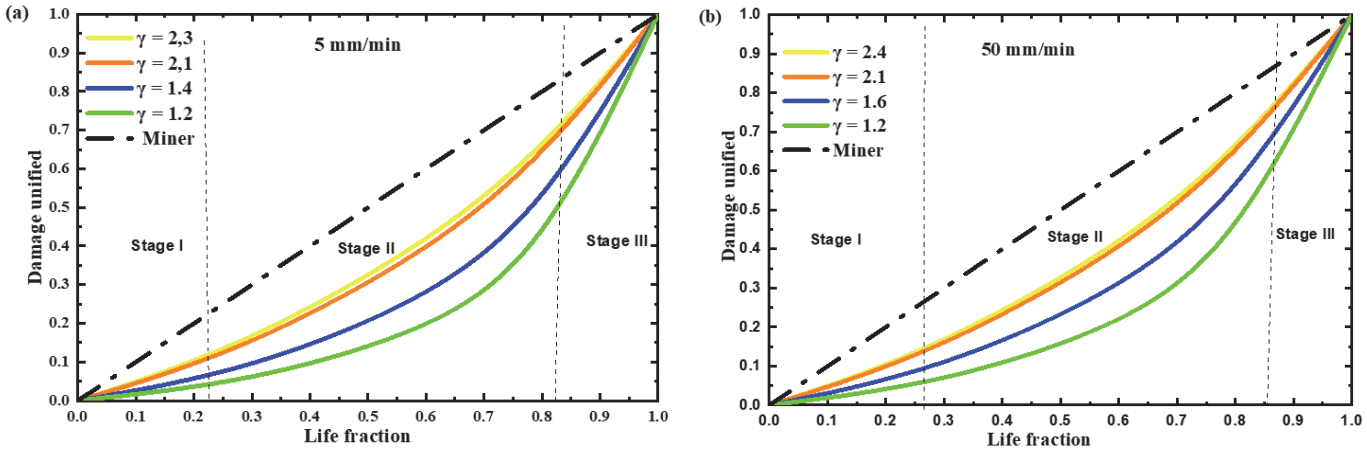

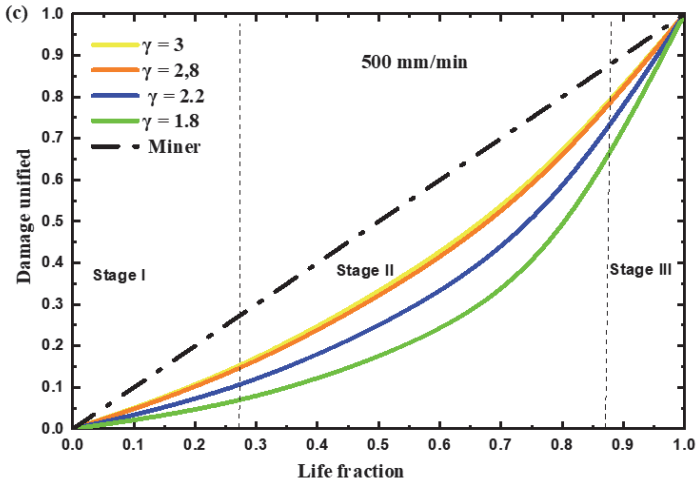

Figure 13: Damage by using the unified model at different temperature and crosshead speed (5(a), 50(b) and 500(c) mm/min).

Conclusion

In this study, the relationship between temperature, crosshead speed, and the mechanical behavior of CPVC samples were studied based on tensile tests at different crosshead speeds and temperatures.

After analyzing and discussing the experimental data and damage models presented, we can be made those tensile properties including Young's modulus and yield stress of chlorinated PVC were shown to be strongly crosshead speed and temperature-dependent. The modulus of elasticity and the yield stress increased with increased crosshead speed at different temperatures and decreased as the temperature increased at different crosshead speeds. The average yield strength increases from around 46 MPa to around 60 MPa when the crosshead speed changes from 5 to 500 mm/min at room temperature and decreases from 59.18 to 18.50 MPa when the temperature changes from -20 to 90°C at 5 mm/min. Then, the establishment of the relationship between damage and reliability enables identification of the critical life fraction and prediction of the ideal moment for transitioning to predictive maintenance.

Additionally, we developed two damage models, one model obtained by adapting the unified theory version and the other quasi-experimental static model based on ultimate stress. Both models, experimental damage and unified suggested, indicated that the initiation, propagation, and acceleration stages of the damage evolution were similar for this material. Comparison of the two models revealed that they adequately described the damage of CPVC, as evidenced by the critical life fraction βc values of 82%, 85%, and 88% for 5, 50, and 500 mm/min, respectively.

References

[1] Wang, J., Xu, H., Battocchi, D., and Bierwagen, G., (2014). The determination of critical pigment volume concentration (CPVC) in organic coatings with fluorescence microscopy. Progress in organic coatings, 77, pp. 2147-2154. DOI: 10.1016/j.porgcoat.2013.12.010.

[2] Elakesh, E.O., Hull, T.R., Price, D., and Carty, P., (2005). Effect of stabilisers and lubricant on the thermal decomposition of chlorinated poly vinyl chloride (CPVC). Polymer degradation and stability, 88, pp. 41-45.

[3] Huang, X., Andry, S., Yaputri, J., Kelly, D., Ladner, D.A., and Whelton, A.J., (2017). Crude oil contamination of plastic and copper drinking water pipes. Journal of hazardous materials, 339, pp. 385-394.

[4] Ren, L., Zhang, S., Zhang, M., Chen, D., and Zhu, F., (2016). The toughness and morphology of chlorinated polyvinyl chloride/(methyl methacrylate-butadiene-styrene) blends. Journal of Vinyl and Additive Technology, 4, pp. 501-505.

[5] Lahlou, M., Kerkour El Miad, A., Nasser, A. and Sadeq, H., (2022). A Study of the Damage Mechanism of Welded CPVC Material. Strength of Materials, 54(6), pp. 1093-1101. DOI: 10.1016/j.prostr.2017.04.041.

[6] El Kori, R., Lamarti, A., Salmi, H., Hachim, A., and El Had, K., (2023). Experimental study of the failure of HDPE and HIPS by the damage's method. Polyolefins Journal. DOI: 10.22063/POJ.2023.3259.1242

[7] Julien, R., Dreelin, E., Whelton, A.J., Lee, J., Aw, T.G., Dean, K., and Mitchell, J., (2020). Knowledge gaps and risks associated with premise plumbing drinking water quality. AWWA Water Science, 2(3), pp.1177.

[8] Kasyanenko, I.M., and Kramarenko, V.Y., (2018). The effect of pigment volume concentration on film formation and the mechanical properties of coatings based on water-dispersion paint and varnish materials. Mechanics of Composite Materials, 53, pp.767-780.
[9] Joshi, G.M., and Deshmukh, K., (2014). Optimized quality factor of graphene oxide-reinforced PVC nanocomposite. Journal of electronic materials, 43, pp.1161-1165. DOI: 10.1007/s11664-014-3010-z.
[10] Merah, N., Irfan-ul-Haq, M. and Khan, Z., (2003). Temperature and weld-line effects on mechanical properties of CPVC. Journal of Materials Processing Technology, 142(1), pp. 247-255. DOI: 10.1016/S0924-0136(03)00567-3.
[11] Liao, Z., Yao, X., Zhang, L., Hossain, M., Wang, J., and Zang, S., (2019). Temperature and strain rate dependent large tensile deformation and tensile failure behavior of transparent polyurethane at intermediate strain rates. International Journal of Impact Engineering, 129, pp.152-167. DOI: 10.1016/j.ijimpeng.2019.03.005.
[12] Reis, J.M.L., Pacheco, L.J., and da Costa Mattos, H.S., (2013). Influence of the temperature and strain rate on the tensile behavior of post-consumer recycled high-density polyethylene. Polymer testing, 32(8), pp.1576-1581. DOI: 10.1016/j.polymertesting.2013.10.008.
[13] Kendall, M.J., and Siviour, C.R., (2014). Rate dependence of poly (vinyl chloride), the effects of plasticizer and time–temperature superposition. Proceedings of the Royal Society A: Mathematical, Physical and Engineering Sciences, 470(2167), pp.20140012. DOI: 10.1098/rspa.2014.0012.
[14] En-naji, A., Mouhib, N., Farid, H., and El Ghorba, M., (2019). Prediction of thermomechanical behavior of acrylonitrile butadiene styrene using a newly developed nonlinear damage-reliability model. Frattura ed Integrità Strutturale, 13(49), pp.748-762. DOI: 10.3221/IGF-ESIS.49.67.
[15] Plaseied, A., and Fatemi, A., (2008). Strain rate and temperature effects on tensile properties and their representation in deformation modeling of vinyl ester polymer. International Journal of Polymeric Materials, 57(5), pp.463-479. DOI: 10.1080/00914030701729677.
[16] Yang, M., Li, W., Dong, P., Ma, Y., He, Y., Zhao, Z., and Chen, L., (2022). Temperature and strain rate sensitivity of yield strength of amorphous polymers: Characterization and modeling. Polymer, 251, pp.124936. DOI: 10.1016/j.polymer.2022.124936.
[17] Gugouch, F., Wahid, A., Bassir, Y., and Elghorba, M., (2023). Fracture analysis of defect Chlorinated Poly Vinyl Chloride pipes based on burst pressure and prediction their fraction of life. Frattura ed Integrità Strutturale, 17(64), pp.218-228. DOI: 10.3221/IGF-ESIS.64.14.
[18] Khtibari, A., El Ouahbi, S., En-Naji, A., Kartouni, A. and El Ghorba, M., (2023). At room temperature, the impact of strain rates on the damage of CVPC compound. Environmental Science and Pollution Research, pp.1-6. DOI: 10.1007/s11356-023-27155-2.
[19] Walley, S.M., Taylor, N.E., and Williamson, D.M., (2018). Temperature and strain rate effects on the mechanical properties of a polymer-bonded explosive. The European Physical Journal Special Topics, 227, pp.127-141. DOI: 10.1140/epjst/e2018-00060-6.
[20] Olufsen, S.N., Nygård, P., Pais, C.I.T., Perillo, G., Hopperstad, O.S. and Clausen, A.H., (2021). Influence of loading conditions on the tensile response of degraded polyamide 11. Polymer, 229, pp.123966. DOI: 10.1016/j.polymer.2021.123966.
[21] Merah, N., Al-Qahtani, T., and Khan, Z., (2008). Effects of strain rate and temperature on tensile properties of CPVC pipe material. Plastics, rubber and composites, 37(8), pp.353-358. DOI: 10.1179/174328908X314352.
[22] Kim, Y., Kim, M.S., Jeon, H.J., Kim, J.H., and Chun, K.W., (2022). Mechanical Performance of Polymer Materials for Low-Temperature Applications. Applied Sciences, 12(23), pp.12251. DOI: 10.3390/app122312251.
[23] Jiang, C., Zhu, Z., Zhang, J., Yang, Z., and Jiang, H., (2020). Constitutive modeling of the rate-and temperature-dependent macro-yield behavior of amorphous glassy polymers. International Journal of Mechanical Sciences, 179, pp.105653. DOI: 10.1016/j.ijmecsci.2020.105653
[24] Lanlan, Z., Yingying, Z., Wei, S., Junhao, X., and Jigang, X., (2021), April. A nonlinear damage constitutive model of PVC coated fabrics. In Structures, 30, pp. 368-377. DOI: 10.1016/j.istruc.2021.01.027.
[25] Hectors, K., and De Waele, W., (2021). Cumulative damage and life prediction models for high-cycle fatigue of metals: a review. Metals, 11(2), pp.204.DOI: 10.3390/met11020204.
[26] Johnson, S., (2014). Thermoelastic stress analysis for detecting and characterizing static damage initiation in composite lap shear joints. Composites Part B: Engineering, 56, pp.740-748. DOI: 10.1016/j.compositesb.2013.09.014.
[27] Quan, D., and Ivankovic, A., (2015). Effect of core–shell rubber (CSR) nano-particles on mechanical properties and fracture toughness of an epoxy polymer. Polymer, 66, pp.16-28. DOI: 10.1016/j.polymer.2015.04.002.
[28] Majid, F., Ouardi, A., Barakat, M., and Elghorba, M., (2017). Mechanical behavior prediction of PPR and HDPE polymers through newly developed nonlinear damage-reliability models. Procedia Structural Integrity, 3, pp.387-394.

DOI: 10.1016/j.prostr.2017.04.043.
[29] Gugouch, F., Sandabad, S., Mouhib, N., and El Ghorba, M., (2019). Prediction of the Lifetime of the Chlorinated PVC Thermoplastic Material Subjected to Thermomechanical Tests-Tensile Test under the Influence of Temperature. In Key Engineering Materials, 820, pp.137-146. DOI: 10.4028/www.scientific.net/KEM.820.137.
[30] Sabah, F., Wahid, A., Nassih, F., El Ghorba, M. and Chakir, H., (2019). Prediction of the lifetime of Acrylonitrile Butadiene Styrene (ABS), by calculation of damage by two methods: damage based on residual stresses and damage bystages evolution. In Key Engineering Materials, 820, pp.203-211. DOI: 10.4028/www.scientific.net/KEM.820.203
[31] Dar, U.A., Zhang, W., Xu, Y., and Wang, J., (2014). Thermal and strain rate sensitive compressive behavior of polycarbonate polymer-experimental and constitutive analysis. Journal of Polymer Research, 21, pp.1-10.
[32] Majid, F., Ouardi, A., Barakat, M., and Elghorba, M., (2017). Mechanical behavior prediction of PPR and HDPE polymers through newly developed nonlinear damage-reliability models. Procedia Structural Integrity, 3, pp.387-394. DOI: 10.1016/j.prostr.2017.04.043.
[33] Youssef, B., Meknassi, M., Achraf, W., Gugouch, F., Lasfar, S., Kane, C.S.E., Kartouni, A., and Elghorba, M., (2023). The analysis of the corrosion effect on the wires of a 19* 7 wire rope by two methods. Engineering Failure Analysis, 144, pp.106816. DOI: 10.1016/j.engfailanal.2022.106816.
[34] Wahid, A., Mouhib, N., Ouardi, A., Sabah, F., Chakir, H. and ELghorba, M., (2019). Experimental prediction of wire rope damage by energy method. Engineering Structures, 201, pp.109794. DOI: 10.1016/j.engstruct.2019.109794.